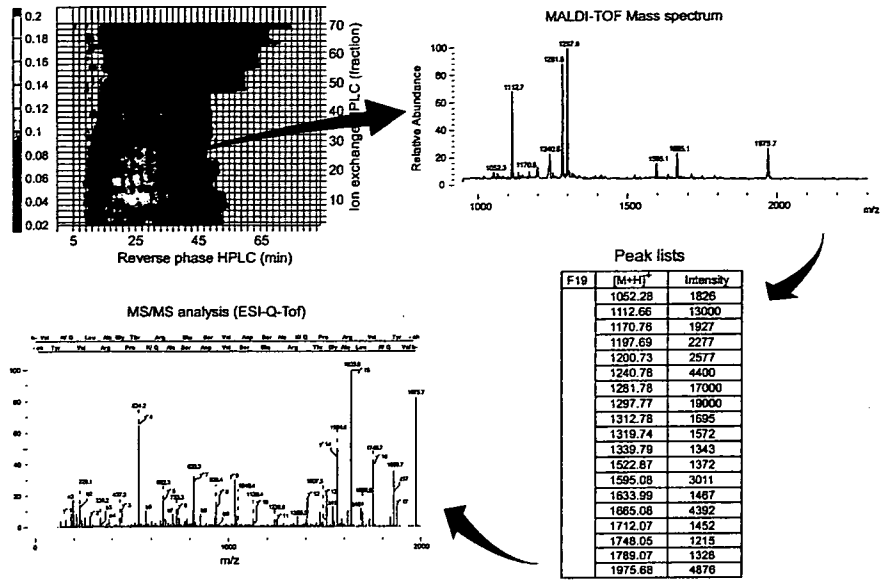

F19	$[M+H]^+$	Intensity
	1052.28	1826
	1112.66	13000
	1170.76	1927
	1197.69	2277
	1200.73	2577
	1240.78	4400
	1281.78	17000
	1297.77	19000
	1312.78	1695
	1319.74	1572
	1339.79	1343
	1522.87	1372
	1595.08	3011
	1633.99	1467
	1665.08	4392
	1712.07	1452
	1748.05	1215
	1789.07	1328
	1975.68	4876

Figure 1. Profiling procedures of the Peptidome database. Peptides are separated by the 2D-HPLC, and each fraction is submitted to the MS analysis. Major peaks are further analyzed by the tandem mass spectrometers.

the physiocochemical properties of peptides along with other related information [1].

Results and Discussion

Pig and mouse brain were collected immediately after sacrifice, diced and boiled in water for more than 5 min to inactivate proteases. After cooling, peptides were homogenized and extracted with 1 M acetic acid. The crude peptide fraction was prepared by the batch-wise treatment with C-18 resin and SP-Sephadex columns, which was separated by Sephadex G-50 gel filtration to remove remaining proteins. The peptide fraction was devided into two fractions of Mr<3,000 and 3,000<Mr<6,000. Each fraction was separated into 70 fractions by SP-2SW ion exchange HPLC with a linear gradient elution of $HCOONH_4$ (pH 3.8) from 10 mM to 1.0 M in the presence of 10% CH_3CN. Seventy fractions thus obtained were each subjected to reverse phase HPLC on a C-18 column with a linear gradient elution of CH_3CN in the presence of 0.1% trifluoroacetic acid (or formic acid), and separated into 75 fractions. By this 2D-HPLC system, peptides were separated into about 5,000 fractions, and an aliquot of each fraction was submitted to MALDI-TOF mass spectrometric (MS) analysis and peak lists of the peptides were stored. For *de novo* sequencing of the peptides, another aliquot was submitted to ESI-Q-TOF or MALDI-TOF-TOF MS analysis, and these data were stored in the database (Fig. 1).

In the course of the separation and analysis, degrees of hydrophobicity, net positive charges and molecular masses of the peptides are determined and estimated, which are employed as major parameters to register the peptide information in the Peptidome database, in addition to their sequences and names [1]. To normalize the 2D-HPLC system, we use a series of synthetic peptides of 11 amino acids with different numbers of positive charges and different hydrophobicity as standards. The

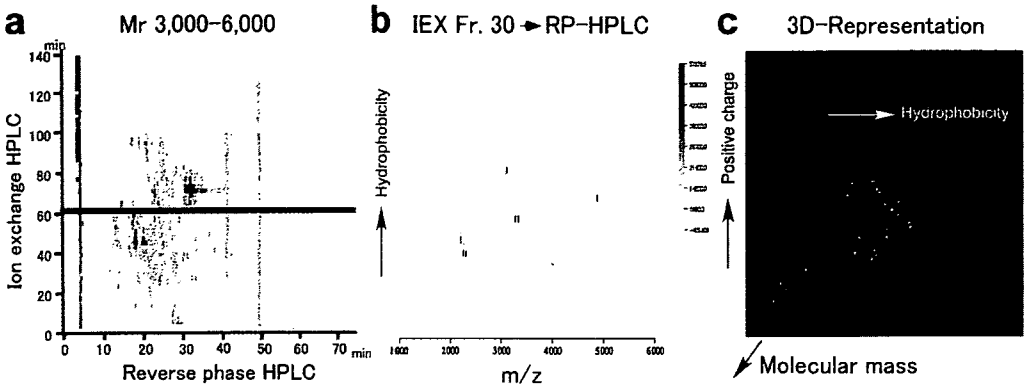

Figure 2. Analysis data for the pig brain peptides of 3,000<Mr<6,000. The peptides were separated by 2D-HPLC (a), analyzed by the mass spectrometers (b), and finally shown in the virtual 3D-space (c).

positive charge is estimated based on the elution times of the standard peptides, and the hydrophobicity is expressed as a percent CH_3CN concentration where the peptide is eluted.

In Fig. 2, the analysis data for the pig brain peptides of 3,000<Mr<6,000 are indicated step by step. Fig. 2a shows the 2D-HPLC profile of the peptides prepared from 5 g equivalents of the tissue. The absorbance at 210 nm is indicated by the density. Fraction 30 eluted at 60-62 min was then separated by reverse phase HPLC and each fraction was analyzed by the MALDI-TOF. MS analysis data of each fraction are serially plotted against m/z in Fig. 2b, and the density indicates the ion count. Bands with different density indicate the peptides. By accumulating 70 figures like the middle panel, all peptides are drawn in the virtual 3D-space composed of hydrophobicity, positive charge and molecular mass, as shown in Fig. 2c. By the aid of the software, we can freely rotate, zoom in and out this 3D drawing. If you click one ball, you will be able to check the peptide data and information so far as it has been sequenced and annotated.

In the case of pig brain peptides, we analyzed 2 g equivalents of the tissue, and detected 6,573 and 10,215 peptides in the Mr<3,000 and 3,000<Mr<6,000 fractions, respectively. As for about 25% of the detected peptides, the structural information is assumed to be obtained by the MS analysis, although a portion of them has been determined. In the case of mouse brain, we have so far analyzed the peptides in the Mr<3,000 fraction using 0.8 g equivalent of the tissue and detected 4,058 peptides. Among them, about 500 peptide sequences have been determined, and these data are available through the web page of the Peptidome project (www.peptidome.org).

In the case of mouse brain peptides, about 20% of the sequenced peptides are derived from the peptide hormone precursors and the secretory proteins. However, most of other peptides are derived from cytoplasmic, nuclear, mitochondorial, membrane proteins and so on. Several examples of the peptide/precursor relationship are shown in Fig. 3. The peptides derived from proenkephalin A, protachykinin and proopiomelanocortin are considered to be cleaved by prohormone convertases (PC), i.e. cleaved at the consecutive basic amino acids. In the cocaine- and amphetamine regulated transcript (CART), the peptide cleaved at the single arginine residues is observed, and many possible degradation products are detected in the case of procholecystokinin. We found that the regular secretory protein is processed in a

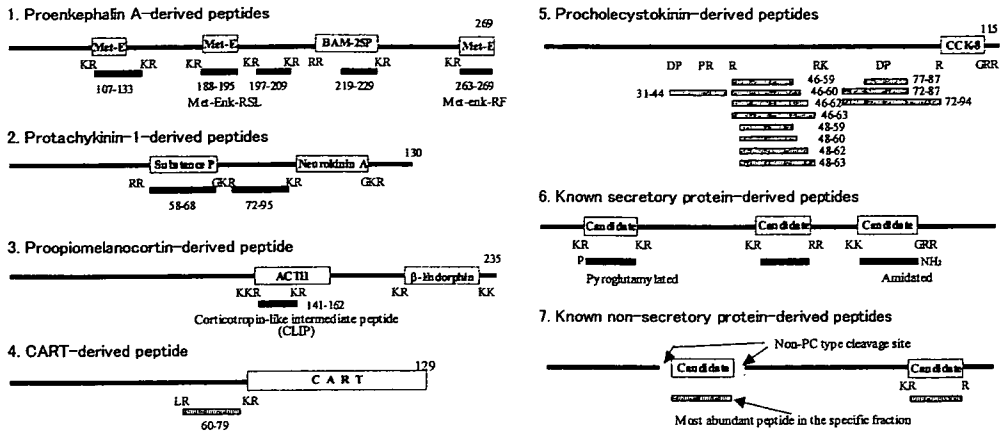

Figure 3. Examples of the peptides identified in the mouse brain extracts. Most peptides derived from the hormone precursor are cleaved by the PCs, but some unique processing patterns are also observed in other cases.

manner similar to that of the peptide hormone precursor. In another case, a unique peptide is present with high abundance but is not flanked by typical processing signals. Although it is necessary to confirm whether these peptides are endogenously present, I am sure that these data will help elucidate endogenous molecular forms and processing profiles of peptides and proteins.

To measure the biological activity, more amounts of peptides are required as compared with those used for the MS analysis even if the highly sensitive screening system is employed. We also separated the pig brain peptides by the large scale 2D-HPLC under the conditions identical to the peptide analysis. An aliquot of each fraction was submitted to the screening, and another aliquot was subjected to the MS analysis to confirm the elution positions. By utilizing the normalized 2D-HPLC as a common platform, data for endogenous peptides, biological activity and their related information can be accumulated, which is expected to increase the chance of discovery of the new bioactive peptides [2,3].

Recently, three groups reported that comprehensive analysis of peptides in the cell, tissue and body fluid can provide valuable information of the endogenous peptides [4-6]. Accumulation of these data in the common database will give us the solid basement for discovery of unidentified endogenous and bioactive peptides.

References

1. Minamino, N., Tanaka, J., Kuwahara, H., Kihara, T., Satomi, Y., Matsubae, M., and Takao, T. (2003) *J. Chromatogr. B*, **792**, 33-48.
2. Katafuchi, T., Kikumoto, K., Hamano, K., Kangawa, K., Matsuo, H., and Minamino, N. (2003) *J. Biol. Chem.*, **278**, 12046-12054.
3. Takeda, S., Okada, T., Okamura, M., Haga, T., Isoyama-Tanaka, J., Kuwahara, H., and Minamino, N. (2004) *J. Biochem.*, **135**, 597-604.
4. Schrader, M. and Schulz-Knappe, P. (2003) *Trends in Biotechnol.*, **19**, S55-S60.
5. Clynen, E., De Loof, A., and Schoofs, L. (2003) *Gen. Comp. Endocrinol.*, **132**, 1-9.
6. Svensson, M., Skold, K., Svenningsson, P., and Andren, P.E. (2003) *J. Proteome Res.*, **2**, 213-219.

循環器病学におけるペプチドミクス

佐々木一樹*，南野直人*
SASAKI Kazuki, MINAMINO Naoto
*国立循環器病センター研究所薬理部

SUMMARY

生理活性ペプチドは循環器疾患の創薬，診断法のシーズとしての有用性が認識されている．ゲノム配列が明らかになった現在も未知の生理活性ペプチドの発見が期待されている．ペプチドミクスは生理活性ペプチドをはじめとした生体に内在するペプチドを包括的に理解するための新しい領域で，現状では発現解析法の確立に主眼が置かれている．新規生理活性ペプチドを発見するためには内在ペプチドの同定が必須であり，それはプロテオミクスでは現実的には不可能である．新規ペプチド発見の新しいアプローチとしてペプチドミクスが市民権を得る時代が到来しようとしている．

POINTS

●循環器疾患の診断・治療法開発のうえでペプチドは今後も有望である．
●ペプチドミクスは，生理活性ペプチド等の生体内に存在するペプチドを対象にする．
●プロテオミクスの手法ではこのようなペプチドは分析できない．
●ペプチドミクスは新規生理活性ペプチド探索の新しいアプローチを提供する．

KEY WORDS

ペプチドミクス，発現解析，生理活性ペプチド，疾患マーカー

はじめに

循環器系の調節因子として，アンジオテンシン，ナトリウム利尿ペプチド類，エンドセリン，アドレノメデュリン（AM）などを標的にした診断・治療法が開発されている．これらは分子量1万以下の小さな蛋白質，すなわちペプチドとよばれる．ペプチドミクスは，生理活性ペプチドをはじめとした生体に内在するペプチドの体系的な解析に関する技術の総称で，循環器病の領域では新規生理活性ペプチドの探索に貢献しうる．内在ペプチドの解析はプロテオミクスでは盲点になっており，本稿ではプロテオミクスとの差異について言及しながら，発現解析のツールとしてのペプチドミクスについて解説するとともに，低分子量蛋白質・ペプチド性の疾患マーカー探索の試みについても紹介する．

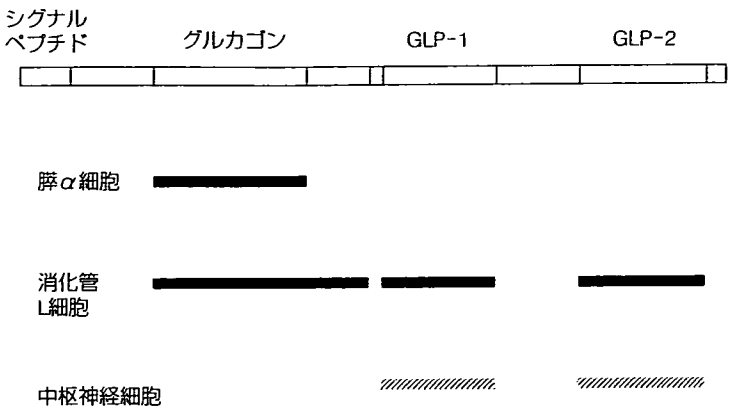

図❶　生理活性ペプチドのプロセシングの多様性
グルカゴンの事例．GLP：Glucagon-like peptide
（筆者作成）

本稿で用いる言葉の定義

ペプチドと蛋白質を区別する明解な定義はないが，一般にはゲル電気泳動で分離，検出されにくい分子量1万以下のアミノ酸のポリマーをペプチドと称する．ペプチドミクスは生体に内在するペプチドの体系的な解析に関する技術で，発現プロテオミクスが対象にしている蛋白質の酵素消化に由来するペプチドは除外される．また，ある系に存在する蛋白質全体をプロテオームと称し，それに対応してペプチド全体をペプチドームと称する．

生体内にどんなペプチドが存在するか

筆者ら[1)~3)]は1999年よりブタ脳を対象にペプチドーム解析を開始した．その結果から推定すると，体内に存在するペプチドの大部分は蛋白質の代謝過程で生じる分解ペプチドであると予想される．そのなかに，「積極的な存在意義」をもったペプチドが微量ながら存在している．医学の立場からは後者，すなわち，特定のアミノ酸配列を認識するプロテアーゼによる切断（プロセシング）に伴って生成するペプチドに興味がもたれる．たとえば，酵素前駆体が活性型に変換される際に随伴して切り出されるプロペプチドや，ペプチドホルモンなどとして知られる生理活性ペプチド，あるいは免疫系細胞のプロテアソームで分解されて主要組織適合性抗原と複合体を形成し抗原提示される10残基程度からなるペプチドなどである．

なかでも，ナトリウム利尿ペプチドやエンドセリンなどの生理活性ペプチドは循環器病の領域で注目される．生理活性ペプチドは，前駆体蛋白質から翻訳された後に，特定のアミノ酸配列を認識するプロテアーゼで切り出されて生じる．そして，特有の翻訳後修飾を伴うことが多く，ほとんどの事例で，その翻訳後修飾が生理活性の発現に必須である．たとえば，強力な摂食亢進作用以外に，重症心不全に対する心機能改善効果を有するグレリンはそのセリン残基がオクタン酸エステル化されており，血管拡張作用や心筋梗塞後の組織保護作用を示すAMは分子内環状構造とアミド化構造を有する．ゲノム情報のみではこのような翻訳後修飾や，組織ごとに異なるプロセシングパターン（図❶）は予測できず，構造解析も含めた発現解析の重要性を示している．したがって，ヒトでゲノム構造がほぼ明らかになったとはいえ，未知の生理活性ペプチドが今後も多数発見されると予想される．

ペプチドミクスとは

ペプチドミクスについて説明する前に，プロテオミクスについて簡単に言及する．これは蛋白質の個別研究ではなく，特定の系に存在する全蛋白質を対象にした発現解析や，構造と機能の相関を体系的に解析するための諸技術を示す言葉である．

一方で，ペプチドミクスは言葉自体が新しく，プロテ

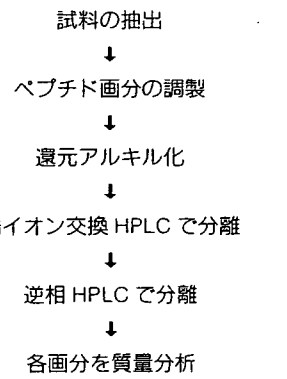

図❷ ペプチドミクスを用いる発現解析の流れ
（筆者作成）

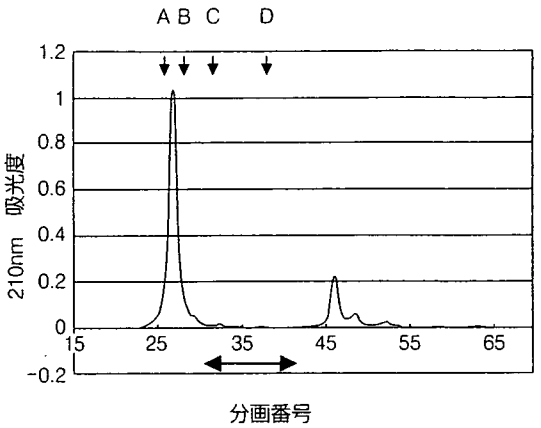

図❸ 培養細胞の上清を逆相系樹脂で処理した試料のゲル濾過
両矢印の領域がペプチド画分に相当する．左側のピークは蛋白質，右側は低分子物質．縦矢印は，分子量マーカーの位置：A，血清アルブミン（約 66,000）；B，RNase A（約 13,500）；C，神経ペプチド Y（4,271）；D，ニューロテンシン（1,673）
（筆者作成）

オミクスと同一視されやすい．現在は内在ペプチドの発現解析がペプチドミクスの最も大きな課題であり，生理活性ペプチドの新しい探索法として今後が期待されている．発現解析の流れを図❷に示す．試料ペプチドを高速液体クロマトグラフィ（high performance liquid chromatography：HPLC）で分離し，各分画の質量分析をおこない，含有されるペプチドの一次構造決定はタンデム質量分析とよばれる手法で進めていく．質量分析計および周辺技術の発展がペプチドミクスの中核をなしている．

ペプチドミクスとプロテオミクスの相違点

発現解析の領域に限定すると，プロテオミクスとペプチドミクスの端的な違いは，ペプチドミクスでは①分析試料から蛋白質成分を分離除去する，②分析試料は酵素消化を実施しない，の 2 点にある．

まず，①の背景について述べる．生物試料に含まれるペプチド総量は，蛋白質総量にくらべて非常に少ない．ブタ脳組織を対象とした筆者らの解析では，ペプチド画分の総重量は蛋白質画分の 0.1%程度であった．ほかの生物試料でも状況は同様である．図❸は，細胞の培養上清の事例で，ペプチドは蛋白質にくらべて少ないことが実感される．質量分析法で検出する場合，共存成分との相対的存在量比によって，当該分子の検出は大きく左右される．したがって発現解析に際してペプチド試料への蛋白質の混入はできうるかぎり排除する必要がある．蛋白質とペプチドの分離は，ゲル濾過，電気泳動ゲルからの electroelution，限外濾過などの方法がある．

つぎに②について説明する前に，プロテオミクスで酵素消化をおこなう理由を述べる．現在の質量分析計では，分子量の制約により，蛋白質自体をタンデム質量分析できないため，酵素消化が実施される．酵素消化にはトリプシンや LysC のように塩基性アミノ酸の C 末端側で切断する酵素が用いられるが，それによって構造解析（タンデム質量分析）時のデータ解釈が多少容易となる．ペプチドミクスはこのような酵素消化を加えることができない．生理活性ペプチドは塩基性アミノ酸を配列中に含むため，このような酵素で切断すると，ペプチド全体の構造を同定できなくなるからである（図❹）．

検出

前述のように，HPLC で分離された試料の質量分析がペプチドの発現解析の主要な作業を占めている．質量分析は高感度でペプチドを検出でき，ペプチドによっては 10 fmol という微量で検出可能である．しかし，これは実際の試料では実現しにくい状況である．たとえば，目的ペプチドを単一状態で 10 fmol 含む試料で良好な s/n で

[MKSIYFVAGLFVMLVQGSWQ] QDTEEKSRSLRSFSASQADPLSDPDQMNEDKRHSQGTFTSDYSKYLDSRR
AQDFVQWLMNTKRNRNNIAKRHDEFERHAEGTFTSDVSSYLEGQAAKEFIAWLVKGRGRRDFPEEVAIVEEL
GRRHADGSFSDEMNTILDNLAARDFINWLIQTKITDRK

図❹　生理活性ペプチド前駆体のアミノ酸配列
グルカゴンの事例．太文字は生理活性ペプチドとして切り出される領域．括弧内はシグナルペプチド．プロテオミクスの手法では，酵素消化が必須のため，図中のRおよびKのC末端側で切断されてしまう．
(筆者作成)

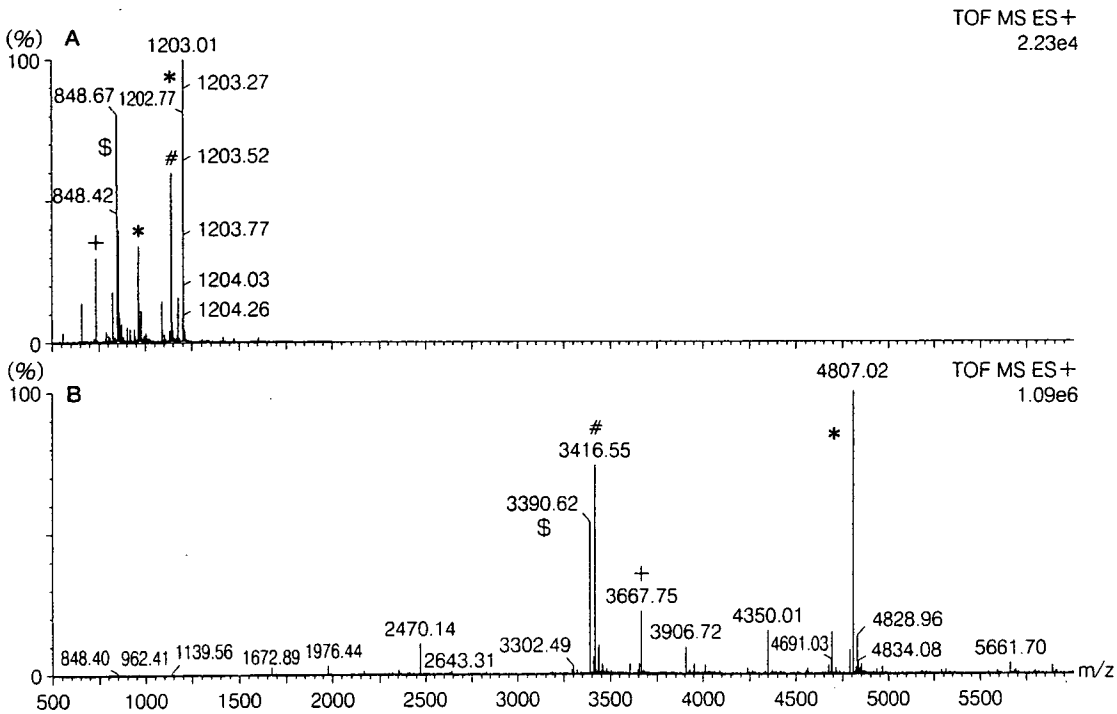

図❺　ESIによるマススペクトルの実際
A：測定で得られるスペクトル．B：Aで観測されるピークを1価に換算したスペクトル．たとえば，Bの＊印で示したペプチドは実際に検出されるわけではなく，実際にはAでみられるように4価，5価イオンのみが観測されている．同様に，Bで#印で示したペプチドは3価イオンのみが観測されている．
(筆者作成)

ピークが観測されたとしても，数十pmolで別のペプチドが共存すると，目的ペプチドの検出強度が顕著に低下する．この現象はイオン抑制とよばれる．イオン抑制効果を最小限にするためには，HPLCを用いてさまざまなパラメータでペプチドを分離する必要がある．

イオン化法は，マトリックス支援レーザー脱離イオン化（matrix assisted laser desorption/ionization：MALDI）と，エレクトロスプレーイオン化（electrospray ionization：ESI）の2種類を併用すると，検出ペプチド数を増加できる．質量分析ではマススペクトルのかたちでデータが得られ，横軸は質量電荷比（m/z），縦軸は相対強度を示す．一般にMALDIでは1価のイオンが強く観察されるために，スペクトル中にどんなペプチドが検出されているか理解しやすい．一方で，ESIでは多価イオンを生じるため，スペクトルは複雑になるのが難点である（図❺）．

同定

検出されたペプチドは逐次同定していく．質量分析計

を用いる一次構造決定法がいくつかあるなかで，タンデム質量分析法が最も実用的である．タンデム質量分析法とは，目的分子をさまざまな方法で断片化させ，生成するイオン（フラグメントイオン）を質量分析して，本来の分子の構造を明らかにする方法である．ヒトのようにゲノム構造がほぼ明らかになった生物種では，タンデム質量分析法による一次構造の決定は，Edman分解およびそれに引きつづくcDNAクローニングに依存していた従来とは比較にならないほど簡便になった．たとえば，図❻では，タンデムマススペクトル上に現れた5つのアミノ酸残基に由来するピークの質量の値，アミノ酸配列，目的ペプチドの質量の情報のみで一意的に同定されている．

タンデム質量分析による同定の実用面での最大の長所は，目的ピークが単一に精製されている必要がないことである．たとえば，図❼の試料中には38種類のペプチドが含まれているが，生化学的な分離操作を加えずに30種類が同定された．Edman分解で問題になるN末端のブロックなどの影響も受けない．ただし，タンデム質量分析法は一種の「破壊分析」であり，目的分子が断片化しない場合や，断片化で生じるフラグメントイオンの情報が不十分な場合は同定不可能である．

ペプチドミクスによる発現解析の実際

発現解析に際しては，試料調製の成否が解析結果の質を左右する．生物試料にはプロテアーゼが多量に含まれ，抽出の過程でペプチドは分解されやすい．また，抽出の過程で蛋白質が分解すると，本来存在していた内在性ペプチドと区別が不可能になる．そこで，これらを抑制するために，組織の場合は迅速な加熱処理，凍結不可避の場合は粉末化後の煮沸，液体試料の場合は迅速な酸処理や蛋白質との分離などで，プロテアーゼを失活，除去させる．また，ジスルフィド結合で環状化した内側のアミノ酸配列情報をタンデム質量分析で得るためには，システイン残基の還元アルキル化が必須である．また，生体試料に含まれる塩類や，化学反応に用いる試薬はペプチドよりイオン化しやすく，ペプチドの検出を妨げるので質量分析前に除去する．

このように調製した試料中には，種類，含有量ともに多種多様なペプチドが混合状態で存在している．これらを可能なかぎり数多く同定することが，発現解析の重要な課題となる．そのためには，原理の異なる液体クロマトグラフィを組みあわせて試料を分離する．1分画に，ある程度の高いs/nをもつペプチドが数種類のみ再現性よく分離されれば理想的であるが，ペプチドによって存在量はさまざまで，その開きは優に10の6乗を超えるため，存在量が多いペプチドは複数の分画に分散する．相対的に存在量が少ないペプチドを同定するためには，もう一段階のHPLC操作を加える．現実的には，ゲル濾過で得られたペプチド画分をまとめて還元アルキル化処理をおこなった試料を引きつづきイオン交換HPLCで分離する．イオン交換HPLCの各分画を逆相HPLCで約50〜100分画に分離する．

このように，原理の異なる2つのクロマトグラフィで分離することを，二次元クロマトグラフィと称する．筆者らは，マウス脳のペプチドーム解析では，脳組織0.8gより出発して，一次元目に陽イオン交換HPLC（70画分），二次元目に逆相HPLC(75画分)，すなわち全体を約5,000画分に分割している．このときに約8,000個のペプチドを検出し，構造決定に至ったのは約1,000個だった．このようにHPLC操作を1つ加えると，解析すべき試料数は飛躍的に増加するため，現実的には，スクリーニングの「網目」をどの程度の細かさ・粗さにするかを試料ごとに検討する必要がある．

候補ペプチドの選択

同定されたペプチドのなかから，生理活性ペプチドに特徴的な翻訳後修飾，同定ペプチドに隣接するアミノ酸配列(切断酵素の認識配列)，ジスルフィド結合，アミノ酸組成をもとに，候補ペプチドを選択する．翻訳後修飾を有する候補分子の場合は，修飾構造選択的な抗体を作製する．免疫染色で当該ペプチドの分布，産生細胞を把握し，さらにそのペプチドが組織中に実在することを，放射免疫測定法（radioimmunoassay：RIA），および組織抽出物からの免疫沈降物の質量分析で確認する．RIAは高感度で定量性にすぐれている．後者はそれらの点では劣っているが，「免疫活性」の実体を理解できる点です

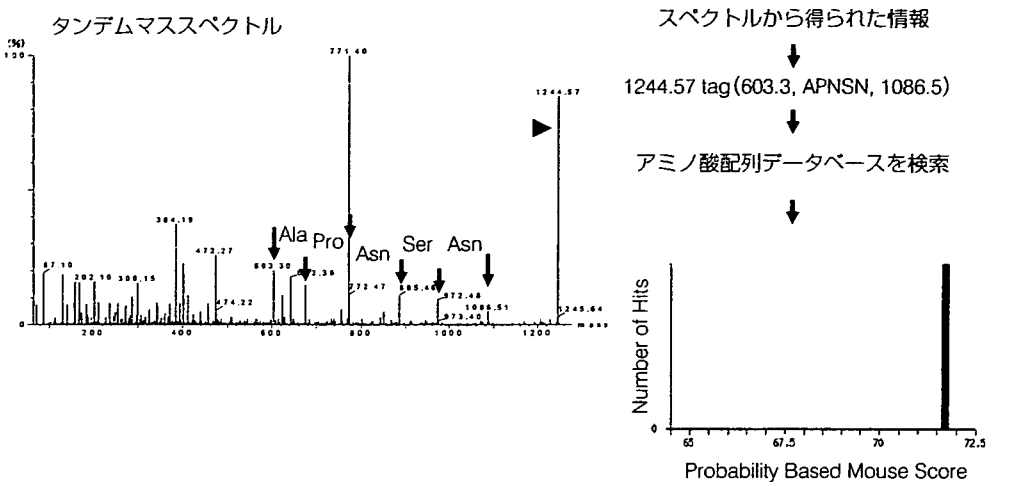

1. gi|4507243　Mass：12727　Total score：72　Peptides matched：1

somatostatin[Homo sapiens]

	Observed	Mr (expt)	Mr (calc)	Delta	Score	Peptide
1	1244.57	1243.56	1243.56	0.00	72	SA**NSNPA**MAPRE

図❻　m/z 1244.57（矢頭）のタンデム質量分析による同定
スペクトル上から連続した 5 つのアミノ酸配列を読み取り，質量の情報とともにデータベースを検索した．太文字の配列を含むペプチドとして一意的に同定された．
（筆者作成）

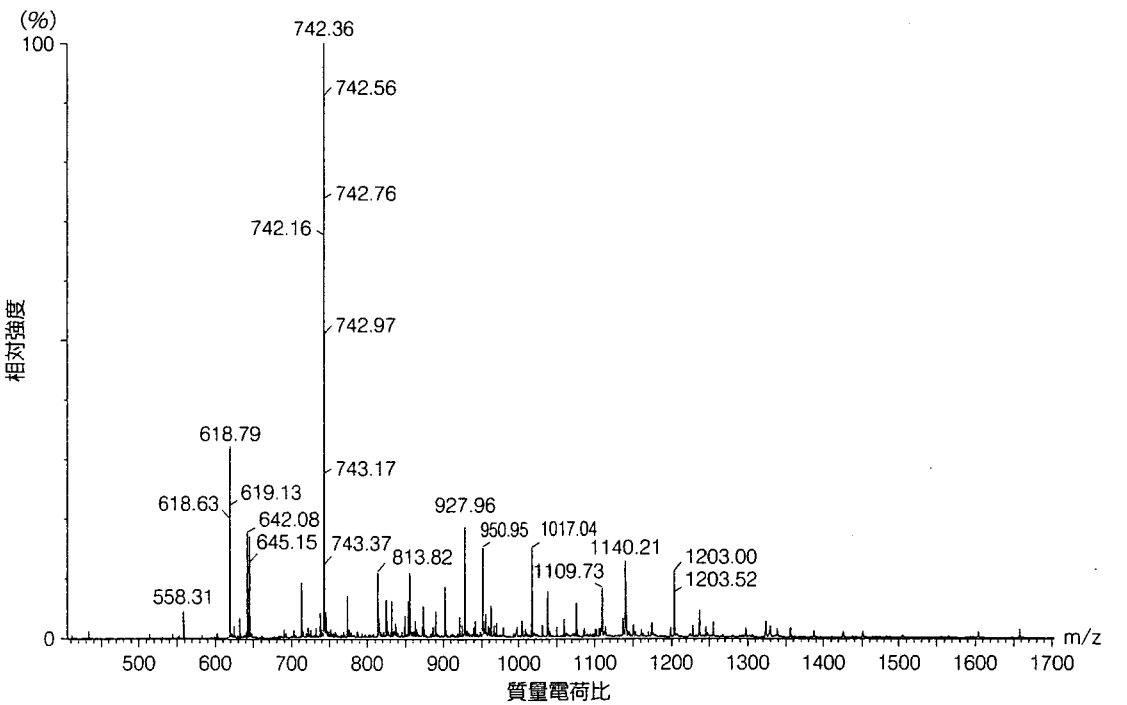

図❼　ペプチドミクスで実際に解析する試料の測定例
質量が測定できた 38 種類のペプチドのうち 30 個はこの試料からタンデム質量分析で同定された．
（筆者作成）

ぐれている[4].

実在を確認後に，どのような活性を有するかを検討する．特定の活性を指標に単離精製して発見されたペプチドとは異なり，この点は試行錯誤の要素が大きくなる．ただし，免疫染色で陽性となる細胞，組織の機能，あるいはその産物から，当該ペプチドの機能は推定も可能である．また，候補ペプチドについて，オーファン受容体のリガンドスクリーニングは受容体同定を考えるうえで望ましい．

上述の方法とは異なり，二次元に分離した各分画について，特定の生物活性で評価する方法も可能性があるが，多量に存在する既知の生理活性ペプチドが複数の分画に分散すると，未知の生理活性ペプチドの活性はマスクされる可能性が強く，工夫を必要とする．候補ペプチドが循環器系に作用するか否かは，生理学的実験が必須であり，動物実験を経て，有用なペプチド候補を選択していく．

疾患マーカーの開発

最後に，低分子量蛋白質関連でとりわけ癌研究で活発に実施されている疾患マーカー探索開発について簡単に言及する．循環器疾患においても，とくに心疾患に関しては診断および治療方針の決定などに有用なマーカーの開発が望まれている．心不全の病態把握のマーカーとして血漿中 BNP 濃度の測定が保険適用になっており，生命予後の予知因子としても確立している．このようなマーカーがさらに発見され，複数のマーカーの測定によって個別的な診断が可能になれば臨床的意義は大きい．究極的にはプアリスク群を選択可能なマーカーが発見されれば望ましい．心筋細胞から分泌あるいは逸脱してくる蛋白質やペプチドは循環血中で希釈されるため，数百 μl の血液検体からこのようなマーカーのプロテオミクス，ペプチドミクスによる探索は現実的には困難である．

これに対して，癌の領域で提唱されたアプローチであるが，血中に多量に存在する蛋白質の数種類の特異的断片のセットが，診断に利用可能であるという成績が多数報告されている[5][6]．これは，癌では早期から凝固，線溶系に異常をきたす場合が多いので，血中に多量に存在する蛋白質にも二次的に影響を与えた結果，スペクトルに変化が現れるのではないかと推定されている．このようなセットを選択するためにはバイオインフォマティクスのソフトウエアの支援が必要になる．循環器疾患の病態に適用可能か否かは今後の課題になるが，その検討には，表面改良型レーザー脱離イオン化質量分析法[6] (surface-enhanced laser desorption/ionization：SELDI) やアルブミンに非共有結合的に付着している低分子蛋白質を分析するアプローチが欧米では実施されている[7]．血清は凝固の過程で多数のプロテアーゼが活性化されており，多数のペプチド性ピークが観測されたとしても，真の病態を反映しているか，採血以後の体外で生じたアーティファクトなのかについて，試料の採取を含めた厳格な管理が必須となる[8]．

おわりに

本稿ではプロテオミクスと混同されやすいペプチドミクスについて，総論的な解説を中心にすえながら，運用面での注意点についても言及した．ペプチドミクスが循環器病領域で期待される役割として現在のところ中心になっているのは，新規生理活性ペプチドの探索と疾患マーカー開発である．本稿がその現状について理解するための一助になれば幸いである．

文　献

1) 南野直人：ペプチドーム―生体内ペプチドのファクトデータベース化―．蛋白質核酸酵素 46 (suppl 11)：S 1510-S 1517，2001
2) Minamino N *et al*：Determination of endogenous peptides in the porcine brain：possible construction of peptidome, a fact database for endogenous peptides. *J Chromatogr B Analyt Technol Biomed Life Sci* 792：33-48, 2003
3) 佐々木一樹ほか：ペプチドーム解析の現状と展望．実験医学増刊 23：133-140，2005
4) Sasaki K *et al*：Peptidomics-based approach reveals the

secretion of the 29-residue COOH-terminal fragment of the putative tumor suppressor protein DMBT1 from pancreatic adenocarcinoma cell lines. *Cancer Res* 62：4894-4898, 2002

5) Li J *et al*：Proteomics and bioinformatics approaches for identification of serum biomarkers to detect breast cancer. *Clin Chem* 48：1296-1304, 2002

6) 佐々木一樹：SELDI-TOF-MSによる腫瘍マーカー探索とがん診断の試み．化学フロンティア10，化学同人，京都，2003，pp. 181-190

7) Stanley BA *et al*：Heart disease, clinical proteomics and mass spectrometry. *Dis Markers* 20：167-178, 2004

8) Tammen H *et al*：Peptidomic analysis of human blood specimens：comparison between plasma specimens and serum by differential peptide display. *Proteomics* 5：3414-3422, 2005

SASAKI Kazuki

ささき・かずき
北海道生まれ．東京大学医学部医学科卒，国立がんセンター研究所を経て，2004年より国立循環器病センター研究所．
研究テーマ：質量分析法による新規生理活性ペプチドの探索．
趣味：音楽・庭園鑑賞．
E-mail：ksasaki@ri.ncvc.go.jp

Available online at www.sciencedirect.com
SCIENCE DIRECT®
Biochemical and Biophysical Research Communications 330 (2005) 75–80
BBRC
www.elsevier.com/locate/ybbrc

Calcitonin receptor-stimulating peptide-1 regulates ion transport and growth of renal epithelial cell line LLC-PK$_1$

Kazumasa Hamano, Takeshi Katafuchi, Katsuro Kikumoto, Naoto Minamino *

National Cardiovascular Center Research Institute, 5-7-1 Fujishirodai, Suita, Osaka 565-8565, Japan

Received 18 February 2005

Abstract

Calcitonin receptor-stimulating peptide-1 (CRSP-1) is a peptide recently identified from porcine brain by monitoring the cAMP production through an endogenous calcitonin (CT) receptor in the renal epithelial cell line LLC-PK$_1$. Here we investigated the effects of CRSP-1 on the ion transport and growth of LLC-PK$_1$ cells. CRSP-1 inhibited the growth of LLC-PK$_1$ cells with a higher potency than porcine CT. CRSP-1 enhanced the uptake of $^{22}Na^+$ into LLC-PK$_1$ cells more strongly than did CT and slightly reduced the $^{45}Ca^{2+}$ uptake. The enhancement of the $^{22}Na^+$ uptake was abolished by 5-(*N*-ethyl-*N*-isopropyl) amiloride, a strong Na^+/H^+ exchanger (NHE) inhibitor for NHE1, even at a concentration of 1×10^{-8} M, although other ion transporter inhibitors did not affect the $^{22}Na^+$ uptake. These results indicate that CRSP-1 enhances the $^{22}Na^+$ uptake by the specific activation of NHE1. Taken together, CRSP-1 is considered to be a new regulator for the urinary ion excretion and renal epithelial cell growth.

Keywords: Calcitonin receptor-stimulating peptide; Calcitonin; Calcitonin receptor; cAMP; LLC-PK$_1$ cell; Na^+/H^+ exchanger; 5-(*N*-Ethyl-*N*-isopropyl) amiloride; cAMP-dependent protein kinase

Calcitonin receptor-stimulating peptide-1 (CRSP-1) is a strong and specific agonist for the calcitonin (CT) receptor, its stimulatory activity for the cAMP production is 10-fold and more than 100-fold stronger than porcine CT in LLC-PK$_1$ cells and COS-7 cells expressing the CT receptor, respectively [1].

Measurement of CRSP-1 concentration in various porcine tissues by radioimmunoassay showed that the pituitary gland and thyroid gland contain the highest levels of CRSP-1 in the pig, although this peptide is widely distributed throughout the central nervous system. In the in vivo experiment, the bolus administration of CRSP-1 into rats significantly reduced the plasma Ca^{2+} level. We assumed that the CRSP-1 secreted from the pituitary gland and thyroid gland into the systemic circulation stimulated the CT receptor and regulated the physiological events in the kidney and the bone. Thus, we focused on the effect of CRSP-1 on the renal function in this study. LLC-PK$_1$ is one of the most characterized renal tubular epithelial cell lines [2–4]. This cell line abundantly expresses the CT receptor [5] and is often used for the analysis of the cell physiological function of CT in the renal epithelial cells. As CRSP-1 stimulates the cAMP production in LLC-PK$_1$ cells more potently than does CT, we examined the effect of CRSP-1 on LLC-PK$_1$ cells to elucidate the cell physiological function of CRSP-1 in the renal epithelial. In this study, therefore, we investigated the effects of CRSP-1 on ion uptake into LLC-PK$_1$ cells and their growth.

Materials and methods

Materials. Synthetic CRSP-1 and salmon CT were prepared and purchased as described previously [1]. ^{125}I-labeled deoxybromouridine (^{125}I-DU), ^{22}NaCl, and $^{45}CaCl_2$ were purchased from Amersham

* Corresponding author. Fax: +81 6 6835 5349.
E-mail address: minamino@ri.ncvc.go.jp (N. Minamino).

0006-291X/$ - see front matter © 2005 Elsevier Inc. All rights reserved.
doi:10.1016/j.bbrc.2005.02.131

Biosciences (Buckingham, UK). Benzthiazide, furosemide, 4-acetamido-4′-isothiocyanostilbene-2,2′-disulfonic acid (SITS), bumetanide, and 5-(*N*-ethyl-*N*-isopropyl) amiloride (EIPA) were purchased from Sigma (St. Louis, MO, USA).

Cell culture. LLC-PK_1 cells and opossum kidney (OK) cells were cultured with Dulbecco's modified Eagle's medium (DMEM) and minimum essential medium, respectively, supplemented with 10% fetal bovine serum (FBS), 100 μg/ml penicillin, and 100 U/ml streptomycin in a humidified atmosphere of 95% air–5% CO_2 at 37 °C.

Measurement of cAMP production in LLC-PK_1 cells. LLC-PK_1 cells were harvested, seeded at a density of 1×10^5 cell/well on 48-well plates, and cultured for 24 h. The cells were washed twice with DMEM/Hepes (20 mM, pH 7.4) containing 0.5 mM of 3-isobutyl-1-methyl xanthine (IBMX, Sigma) and 0.05% bovine serum albumin (DMEM/Hepes/IBMX solution), and were incubated in the same medium for 30 min at 37 °C. The incubation medium was then replaced with 150 μl medium, in which the sample of interest was dissolved, and further incubated at 37 °C for another 30 min. Aliquots (100 μl) of the incubation media were succinylated, evaporated, and then submitted to radioimmunoassay for cAMP, as reported previously [1].

Measurement of ^{125}I-DU uptake into LLC-PK_1 cells. The cells were harvested, seeded at a density of 2×10^4 cell/well on 24-well plates, and cultured for 48 h. The cells at 70% confluence were washed with 0.5 ml serum-free DMEM, replaced with DMEM containing 10% FBS and the peptide of interest, and incubated for 2 h at 37 °C. Then, ^{125}I-DU (4×10^5 cpm/50 μl in the DMEM) was added and further incubated for 5 h at 37 °C. Following the incubation, the cells were washed twice with ice-cold phosphate-buffered saline, incubated on ice for 30 min with 5% trichloroacetic acid, washed twice with 99.5% ethanol, and then solubilized in a buffer containing 0.1 M NaOH, 2% Na_2CO_3, and 1% SDS (500 μl/well). The radioactivity in each well was counted using a γ counter (ARC-1000, Aloka, Tokyo, Japan).

Measurement of intracellular cAMP accumulation in OK cells. OK cells were harvested, seeded at a density of 2×10^5 cell/well on 24-well plates, and cultured for 24 h. Porcine CT receptor cDNA ligated into pcDNA 3.1 expression vector (Promega, Madison, WI, USA) was transfected into the OK cells using Lipofectamine Plus (Invitrogen, San Diego, CA, USA) according to the manufacturer's protocol, and further incubated for 24 h. The cells were washed twice with DMEM/Hepes/IBMX solution and incubated in the same medium for 30 min at 37 °C. The incubation medium was then replaced with 250 μl medium, in which the sample of interest was dissolved, and further incubated at 37 °C for another 10 min. Following the incubation, the medium was replaced with 99.5% ethanol, and the cells were frozen at −80 °C for 24 h. The cells were lysed by repeated pipetting, and the debris of the lysate was removed by centrifuging at 12,000*g* for 5 min. The supernatant was evaporated, and the resulting pellet was dissolved in DMEM/Hepes/IBMX solution. Aliquots (100 μl) of the incubation media were succinylated, evaporated, and then submitted to radioimmunoassay for cAMP as reported previously [1].

Measurement of $^{45}Ca^{2+}$ uptake into LLC-PK_1 cells. LLC-PK_1 cells were harvested, seeded at a density of 2×10^6 cells on 6-well plates, and cultured for 2 days. The cells were washed twice with a calcium-free Hanks' solution, and replaced with the calcium-free Hanks' solution containing $^{45}Ca^{2+}$ (37 kBq/ml), in the absence or presence of CRSP-1 at a concentration of 1×10^{-6} M. Following incubation at 37 °C for 10 min, the cells were washed three times with ice-cold washing buffer (140 mM KCl, 5 mM $MgCl_2$, 20 mM Hepes (pH 7.4), 80 mM sucrose, and 1 mM EGTA), and the radioactivity incorporated into the cells was measured using a Topcount scintillation counter (Packard, Meriden, CT, USA).

Measurement of $^{22}Na^+$ uptake into OK cells and LLC-PK_1 cells. OK cells expressing recombinant CT receptor or LLC-PK_1 cells were harvested, seeded at a density of 2×10^6 cells/well on 6-well plates, and cultured for 2 days. The cells were washed twice with a Hanks'-choline chloride solution (137 mM choline chloride, 5.4 mM KCl, 4.2 mM $NaHCO_3$, 3 mM Na_2HPO_4, 0.4 mM KH_2PO_4, 1.3 mM $CaCl_2$, 0.5 mM $MgCl_2$, 0.8 mM $MgSO_4$, 10 mM glucose, and 5 mM Hepes, pH 7.4). Then, the Hanks'-choline chloride-$^{22}Na^+$ (37 kBq/ml) solution containing CRSP-1 (1×10^{-8} – 1×10^{-6} M) alone, one of ion transporter inhibitors (1×10^{-6} M) alone, CRSP-1 (1×10^{-6} M) and one of ion transporter inhibitors (1×10^{-6} M), or CRSP-1 (1×10^{-6} M) and EIPA (1×10^{8} – 1×10^{-6} M) was administered. Following incubation at 37 °C for 10 min, the cells were washed three times with ice-cold saline, and the $^{22}Na^+$ uptake into the cells was measured using a γ-counter (Cobra 5003, Packard).

Statistical analysis. Statistical analysis was performed using a one-way analysis of variance with repeated measurements, combined with a multiple comparison (Scheffe's *F* test). These analyses were carried out using StatView 5.01 (SAS Institute, Cary, NC, USA). The data are expressed as means ± SEM. *P* values less than 0.05 were considered significant.

Results

Fig. 1A shows the dose-dependent elevation of cAMP levels in the LLC-PK_1 cells stimulated with porcine CRSP-1, salmon CT, and porcine CT. CRSP-1, as well

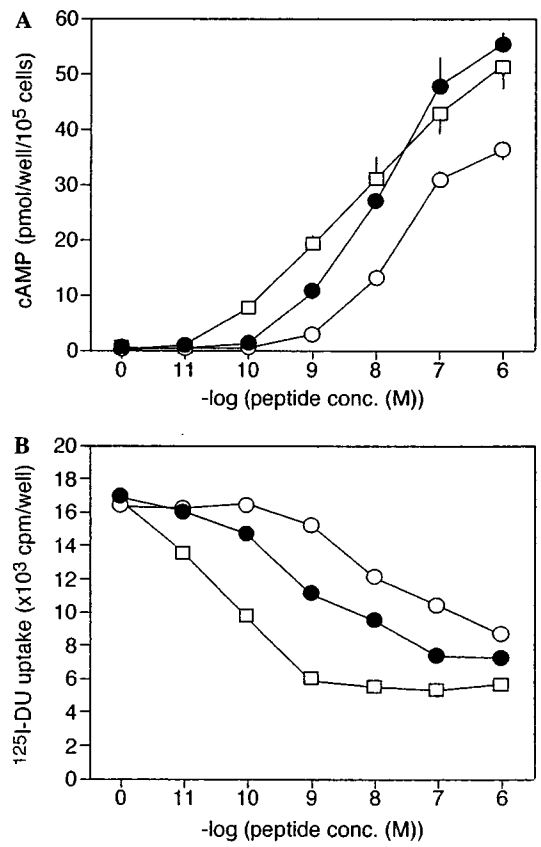

Fig. 1. Effects of CRSP-1, salmon CT, and porcine CT on cAMP production (A) and ^{125}I-DU uptake (B) into LLC-PK_1 cells. The cells were stimulated with porcine CRSP-1 (closed circle), salmon CT (open square) or porcine CT (open circle). (A) Dose-dependent increase of cAMP concentration in the culture medium of LLC-PK_1 cells. (B) Dose-dependent reduction of ^{125}I-DU uptake into LLC-PK_1 cells. Each point represents the mean ± SEM of three separate determinations.

as salmon CT and porcine CT, stimulated the cAMP production, and the potency order of the three peptides in the stimulatory activity of cAMP production was salmon CT > CRSP-1 > porcine CT. Since the increase of the intracellular cAMP concentration induces a change in growth of a variety of cell types, we next evaluated the effect of these peptides on the growth of the LLC-PK_1 cells by measuring the ^{125}I-DU uptake into chromosomal DNA. Parallel to the dose-dependent elevation of the cAMP production, these three peptides reduced the ^{125}I-DU uptake into LLC-PK_1 cells with the order of potency being salmon CT > CRSP-1 > porcine CT (Fig. 1B).

We next investigated the effects of CRSP-1 on ion transport. The effect of CRSP-1 on the $^{45}Ca^{2+}$ uptake into LLC-PK_1 cells is shown in Fig. 2. CRSP-1 significantly but weakly reduced the $^{45}Ca^{2+}$ uptake at a concentration of 1×10^{-6} M, and the effect of CRSP-1 on the reduction was weaker than that of salmon CT. A significant reduction of $^{45}Ca^{2+}$ uptake was not observed when LLC-PK_1 cells were stimulated with CRSP-1 at a concentration of 1×10^{-7} M (data not shown).

Fig. 3A shows the time course of $^{22}Na^{+}$ uptake into LLC-PK_1 cells in the absence or presence of CRSP-1. The $^{22}Na^{+}$ uptake into LLC-PK_1 cells was observed even at 0.1 min and reached a plateau at 60 min. When the cells were stimulated with CRSP-1 at a concentration of 1×10^{-7} M, the $^{22}Na^{+}$ uptake was significantly enhanced at 5 min and the enhancement reached a maximum at 10 min. Based on this result, we incubated the LLC-PK_1 cells with peptides and $^{22}Na^{+}$ for 10 min, and observed the enhancement of $^{22}Na^{+}$ uptake into the cells (Fig. 3B). CRSP-1 enhanced the $^{22}Na^{+}$ uptake into LLC-PK_1 cells from a concentration of 1×10^{-8} M. The potency order of the $^{22}Na^{+}$ uptake-increasing activity was salmon CT > CRSP-1 > porcine CT and was in agreement with that of cAMP production. Thus, we studied the effect of CRSP-1 on the $^{22}Na^{+}$ uptake in greater detail.

To verify that the activation of the CT receptor by CRSP-1 induces $^{22}Na^{+}$ uptake, porcine CT receptor

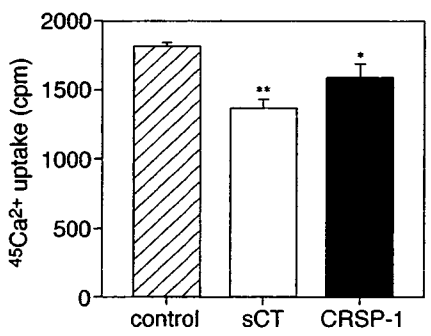

Fig. 2. Effects of CRSP-1, salmon CT, and porcine CT on $^{45}Ca^{2+}$ uptake. The cells were incubated with $^{45}Ca^{2+}$ only (control), with $^{45}Ca^{2+}$ and salmon CT (sCT, 1×10^{-6} M) or porcine CRSP-1 (CRSP-1, 1×10^{-6} M). Each bar represents the mean ± SEM of three separate determinations. $*P < 0.05$; $**P < 0.001$.

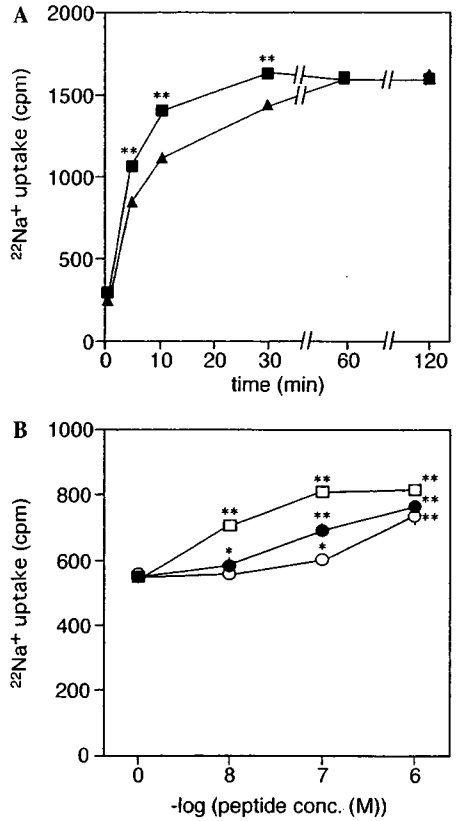

Fig. 3. Time course and dose-dependent enhancement of $^{22}Na^{+}$ uptake into LLC-PK_1 cells. (A) LLC-PK_1 cells were incubated with $^{22}Na^{+}$ in the absence (closed triangle) or presence of 1×10^{-7} M of CRSP-1 (closed square) for 0.1, 5, 10, 30, 60, and 120 min. (B) LLC-PK_1 cells were incubated with $^{22}Na^{+}$ only or with $^{22}Na^{+}$ and the indicated concentrations of porcine CRSP-1 (closed circle), salmon CT (open square), and porcine CT (open circle) for 10 min. Each point represents the mean ± SEM of three separate determinations. $*P < 0.05$; $**P < 0.001$.

cDNA inserted into mammalian expression vector (pcDNA-CTR) was transfected into OK cells, and the $^{22}Na^{+}$ uptake into the cells was measured in the presence of CRSP-1. CRSP-1 stimulated the cAMP production in OK cells, only when pcDNA-CTR was transfected into the cells (Fig. 4A). Parallel to the elevation of cAMP production, the $^{22}Na^{+}$ uptake into OK cells was enhanced with CRSP-1 (Fig. 4B). These results confirm that CRSP-1 actually enhanced the $^{22}Na^{+}$ uptake through the CT receptor-cAMP pathway.

To determine which Na^{+} transporter is activated with CRSP-1, we administered various transporter inhibitors, such as furosemide ($Na^{+}/K^{+}/Cl^{-}$ cotransporter inhibitor), benzthiazide (Na^{+}/Cl^{-} cotransporter inhibitor), EIPA (Na^{+}/H^{+} exchanger inhibitor), SITS (Cl^{-}/bicarbonate exchanger inhibitor), and bumetanide ($Na^{+}/K^{+}/Cl^{-}$ cotransporter inhibitor), into the culture medium of LLC-PK_1 cells at a concentration of 1×10^{-6} M, and measured their effects on the CRSP-1-induced $^{22}Na^{+}$ uptake. Although furosemide, bumetanide, benzthiazide or SITS did not alter the $^{22}Na^{+}$ uptake, EIPA abolished the

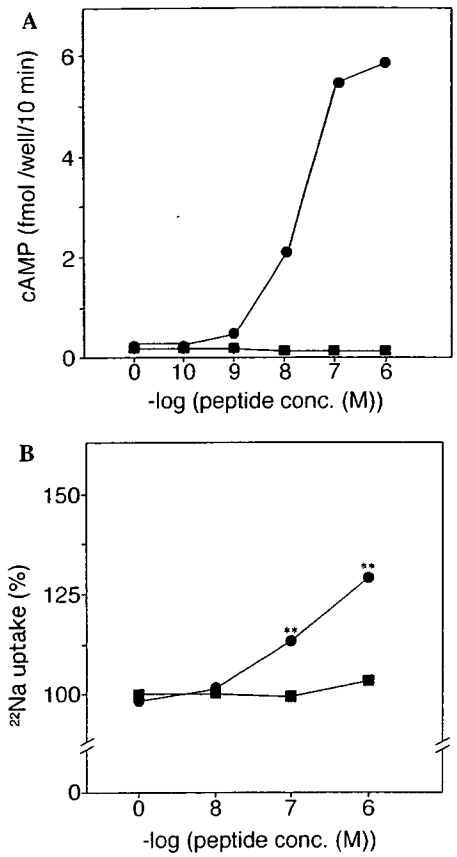

Fig. 4. Effects of CRSP-1 on the intracellular cAMP level (A) and the $^{22}Na^{+}$ uptake (B) into intact OK cells and OK cells transfected with porcine CT receptor. (A) OK cells transfected with porcine CT receptor cDNA (closed circle) and blank vector (closed square) were stimulated with the indicated concentrations of CRSP-1 for 10 min. (B) OK cells transfected with porcine CT receptor cDNA (closed circle) and blank vector (closed square) were incubated with $^{22}Na^{+}$ and the indicated concentrations of CRSP-1 for 10 min. Each point represents the mean ± SEM of three separate determinations. $^{**}P < 0.001$.

effect of CRSP-1 on the $^{22}Na^{+}$ uptake into LLC-PK$_1$ cells (Fig. 5C). These results indicate that the CRSP-1-induced enhancement of $^{22}Na^{+}$ uptake is mediated by a Na^{+}/H^{+} exchanger (NHE).

To identify which isoform of NHEs is responsible for the $^{22}Na^{+}$ uptake that is enhanced by CRSP-1, we treated the cells with different concentrations of EIPA from 1×10^{-8} to 1×10^{-6} M (Fig. 6). The inhibitory effect of EIPA was observed even at a concentration of 1×10^{-8} M. When CRSP-1 and EIPA were administered together at concentrations of 1×10^{-6} M, the effect of CRSP-1 on the $^{22}Na^{+}$ uptake into LLC-PK$_1$ cells was abolished, and the $^{22}Na^{+}$ uptake was reduced to that level when only EIPA had been added to the medium.

Discussion

The effects of CT on renal epithelial cells are known to be mediated by the CT receptor-cAMP pathway [4]. In preceding studies, we demonstrated that porcine CRSP-1 is a more potent and specific agonist for the CT receptor. In the present study, therefore, we investigated the effect of CRSP-1 on the cell physiological events that were induced by the elevation of the cAMP production in the renal epithelial cell line, LLC-PK$_1$.

Fig. 1 shows the anti-proliferative effect of CRSP-1, as well as its stimulatory effect on cAMP production in LLC-PK$_1$ cells, and these effects were 10-fold stronger than those of porcine CT. CT inhibits the growth of LLC-PK$_1$ cells by increasing the intracellular cAMP concentration [6,7]. Jans et al. [6] reported that the growth of LLC-PK$_1$ cells having a mutation in the cAMP-dependent protein kinase (A-kinase) was not inhibited with salmon CT or a vasopressin analogue. Taking these results together, CRSP-1 was deduced to suppress the proliferation of LLC-PK$_1$ through the cAMP-A-kinase pathway.

CRSP-1 and salmon CT reduced $^{45}Ca^{2+}$ uptake into the LLC-PK$_1$ cells (Fig. 2). Several in vivo studies have revealed that urinary Ca^{2+} reabsorption is regulated by the balance between the passive Ca^{2+} influx across the apical membrane via an electrochemical gradient and the active Ca^{2+} extrusion across the basolateral membrane induced with Ca^{2+} pumps and Na^{+}/Ca^{2+} exchangers [8]. Although we cannot specify the target of the CRSP-1-induced suppression of Ca^{2+} uptake, this result raises the possibility that CRSP-1 reduces the plasma Ca^{2+} concentration by inhibiting urinary Ca^{2+} reabsorption into the renal epithelial cells in the kidney.

The $^{22}Na^{+}$ uptake into LLC-PK$_1$ cells was enhanced with CRSP-1 (Fig. 3A). The $^{22}Na^{+}$ uptake into OK cells was enhanced only when the cells expressed recombinant CT receptors (Fig. 4), confirming that CRSP-1 enhances the $^{22}Na^{+}$ uptake into the renal epithelial cells through the CT receptor. As for the mechanism of the CRSP-1-induced enhancement of $^{22}Na^{+}$ uptake into LLC-PK$_1$ cells, this effect was abolished by treating with EIPA, an inhibitor of NHE (Fig. 5) [9]. Two isoforms, NHE1 and NHE3, are expressed in LLC-PK$_1$ cells [10,11], and A-kinase is reported to enhance the NHE1-dependent Na^{+} uptake and to suppress the NHE3-dependent Na^{+} uptake [12,13]. Based on these reports, we at first assumed that the effect of CRSP-1 on the Na^{+} uptake shown in Fig. 3 was the summation of the enhancement of the NHE1-dependent Na^{+} uptake and the suppression of the NHE3-dependent Na^{+} uptake. However, Fig. 6 indicates that CRSP-1 selectively activates NHE1 and enhances Na^{+} uptake, which can be explained by the different 50% inhibitory concentrations of EIPA on NHE1 (approximately 1×10^{-8} M) and NHE3 (more than 1×10^{-6} M) [14–17]. At a concentration of 1×10^{-8} M, EIPA can inhibit 30–40% of the $^{22}Na^{+}$ uptake through NHE1 and cannot inhibit it through NHE3, while at a concentration of 1×10^{-6} M EIPA can inhibit more than 95% of the $^{22}Na^{+}$ uptake

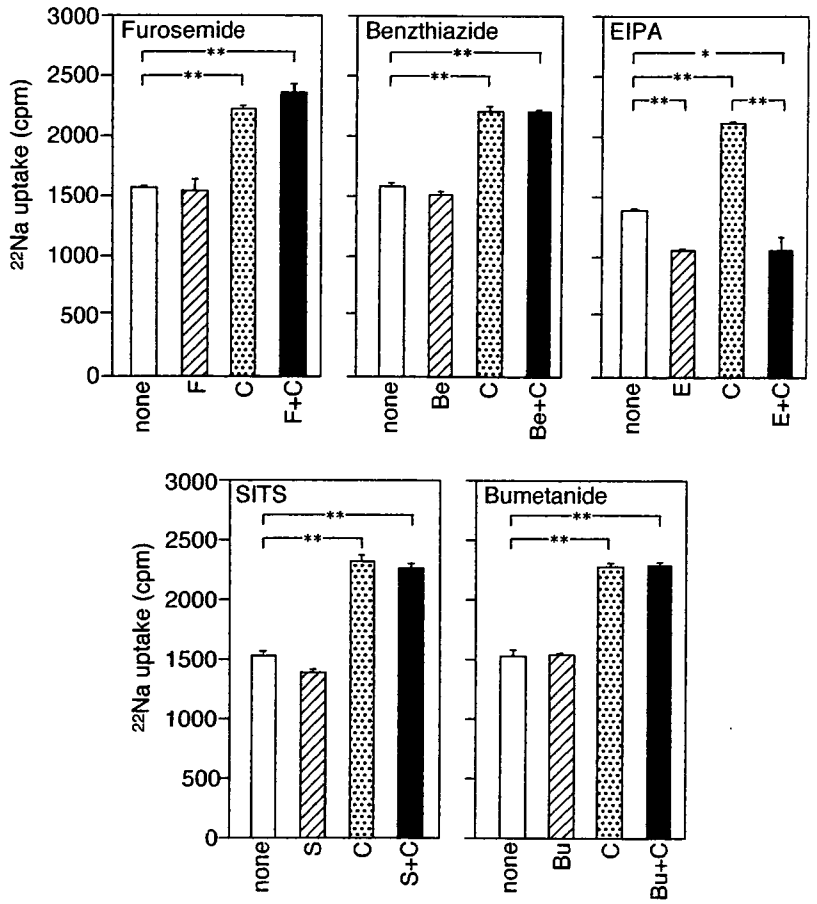

Fig. 5. Effects of ion transporter inhibitors on CRSP-1-induced $^{22}Na^+$ uptake into LLC-PK$_1$ cells. LLC-PK$_1$ cells were incubated for 10 min with none (open bar), 1×10^{-6} M of each ion transporter inhibitor (hatched bar), 1×10^{-6} M CRSP-1 (dotted bar), or 1×10^{-6} M CRSP-1 and 1×10^{-6} M of each ion transporter inhibitor (filled bar), in the presence of $^{22}Na^+$. C, CRSP-1; F, furosemide; Be, benzthiazide; E, EIPA; S, SITS; and Bu, bumetanide. Each bar represents the mean ± SEM of three separate determinations. $^{**}P < 0.001$.

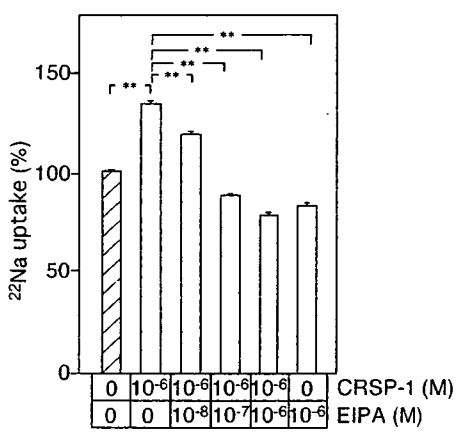

Fig. 6. Dose-dependent inhibitory effect of EIPA on CRSP-1-induced $^{22}Na^+$ uptake into LLC-PK$_1$ cells. LLC-PK$_1$ cells were incubated for 10 min with $^{22}Na^+$ only (hatched bar), or with $^{22}Na^+$ and the indicated concentrations of CRSP-1 and/or EIPA (open bars). Each bar represents the mean ± SEM of three separate determinations. $^{**}P < 0.001$.

through NHE1 and approximately 10% of it through NHE3 [14]. EIPA actually inhibited the CRSP-1-induced enhancement of the $^{22}Na^+$ uptake into the LLC-PK$_1$ cells by about 30% at a concentration of 1×10^{-8} M and abolished it at a concentration of 1×10^{-6} M (Fig. 6). This evidence indicates that CRSP-1 enhanced the $^{22}Na^+$ uptake into LLC-PK$_1$ cells by activating NHE1 and not by suppressing NHE3 under the present experimental conditions.

NHE1 is localized at the basolateral membrane of the epithelial cells [18,19], and elicits many kinds of cell physiological activities, including the regulation of intracellular pH, cell growth, differentiation, cell migration, and cytoskeletal organization [20]. The data obtained in this study confirmed that CRSP-1 regulates NHE1 activity via the CT receptor-A-kinase pathway in the LLC-PK$_1$ cells, suggesting that this peptide can induce NHE1-mediated cell physiological events in the renal epithelial cells.

On the other hand, the NHE3-dependent Na^+ uptake into LLC-PK$_1$ (clone 4) cells was reported to be reduced with salmon CT [21], which indicates that CRSP-1 can reduce NHE3 activity by stimulating the CT receptor. In the LLC-PK$_1$ cells used in this study, however, we observed only the stimulatory effect of CRSP-1 on the NHE1 activity instead of observing its inhibitory effect

on the NHE3 activity, probably due to their much lower NHE3 activity than that of NHE1. As NHE3 is localized at the apical membrane of the epithelial cells and is mainly involved in natriuresis, CRSP-1 may be able to regulate the urinary sodium concentration via NHE3 being expressed in the renal epithelial cells.

In conclusion, we investigated the effects of CRSP-1 on the renal epithelial cell line LLC-PK_1, and showed that CRSP-1 enhances the Na^+ uptake mainly through NHE1, reduces the Ca^{2+} uptake, and inhibits the growth of this cell line. Furthermore, these effects of CRSP-1 are stronger than those of porcine CT, which is in agreement with their potencies toward the CT receptor. While the tissue concentration of CRSP-1 in the thyroid gland is estimated to be about 1/10 that of CT [1,22], CRSP-1 is present at a high concentration in the pituitary gland where CT was not detected. These data indicate that the CRSP-1 secreted from these glands can regulate renal epithelial cells in vivo.

Acknowledgments

This work was supported in part by research grants from the Ministry of Education, Culture, Sports, Science and Technology (Special Coordination Funds for the Promotion of Science and Technology), from the Ministry of Health, Labor and Welfare (Cardiovascular Diseases), from the Pharmaceuticals and Medical Devices Agency (Medical Frontier Project) of Japan, and from the Protein Research Foundation (Kaneko-Narita Research Grant). The authors are grateful to Dr. Wakabayashi of this institute for his helpful discussion, and to Ms. A. Okabe, Y. Takada, and S. Fujiwara of this institute for their technical assistance.

References

[1] T. Katafuchi, K. Kikumoto, K. Hamano, K. Kangawa, H. Matsuo, N. Minamino, Calcitonin receptor-stimulating peptide, a new member of the calcitonin gene-related peptide family. Its isolation from porcine brain, structure, tissue distribution, and biological activity, J. Biol. Chem. 278 (2003) 12046–12054.

[2] R.N. Hull, W.R. Cherry, G.W. Weaver, The origin and characteristics of a pig kidney cell strain, LLC-PK, In Vitro 12 (1976) 670–677.

[3] A. Perantoni, J.J. Berman, Properties of Wilms' tumor line (TuWi) and pig kidney line (LLC-PK_1) typical of normal kidney tubular epithelium, In Vitro 15 (1979) 446–454.

[4] J.S. Handler, F.M. Perkins, J.P. Johnson, Studies of renal cell function using cell culture techniques, Am. J. Physiol. 238 (1980) F1–F9.

[5] H.Y. Lin, T.L. Harris, M.S. Flannery, A. Aruffo, E.H. Kaji, A. Gorn, L.F. Kolakowski Jr., H.F. Lodish, S.R. Goldring, Expression cloning of an adenylate cyclase-coupled calcitonin receptor, Science 254 (1991) 1022–1024.

[6] D.A. Jans, E.L. Gajdas, C. Dierks-Ventling, B.A. Hemmings, F. Fahrenholz, Long-term stimulation of cAMP production in LLC-PK_1 pig kidney epithelial cells by salmon calcitonin or a photoactivatable analogue of vasopressin, Biochim. Biophys. Acta 930 (1987) 392–400.

[7] A. Inoue, Y. Komatsu, J. Ochiai, S. Itagaki, H. Nishide, M. Shikano, H. Hemmi, N. Numao, Growth inhibition and morphological changes of LLC-PK_1 induced by ultimobranchial calcitonins, Cell Biol. Int. Rep. 14 (1990) 887–896.

[8] R.J. Bindels, Calcium handling by the mammalian kidney, J. Exp. Biol. 184 (1993) 89–104.

[9] S. Wakabayashi, M. Shigekawa, J. Pouyssegur, Molecular physiology of vertebrate Na^+/H^+ exchangers, Physiol. Rev. 77 (1997) 51–74.

[10] R.F. Reilly, F. Hildebrandt, D. Biemesderfer, C. Sardet, J. Pouyssegur, P.S. Aronson, C.W. Slayman, P. Igarashi, cDNA cloning and immunolocalization of a $Na^{(+)}$–H^+ exchanger in LLC-PK_1 renal epithelial cells, Am. J. Physiol. 261 (1991) F1088–F1094.

[11] C.A. Shugrue, N. Obermuller, S. Bachmann, C.W. Slayman, R.F. Reilly, Molecular cloning of NHE3 from LLC-PK_1 cells and localization in pig kidney, J. Am. Soc. Nephrol. 10 (1999) 1649–1657.

[12] R.A. Kandasamy, F.H. Yu, R. Harris, A. Boucher, J.W. Hanrahan, J. Orlowski, Plasma membrane Na^+/H^+ exchanger isoforms (NHE-1, -2, and -3) are differentially responsive to second messenger agonists of the protein kinase A and C pathways, J. Biol. Chem. 270 (1995) 29209–29216.

[13] A. Azarani, J. Orlowski, D. Goltzman, Parathyroid hormone and parathyroid hormone-related peptide activate the Na^+/H^+ exchanger NHE-1 isoform in osteoblastic cells (UMR-106) via a cAMP-dependent pathway, J. Biol. Chem. 270 (1995) 23166–23172.

[14] J. Orlowski, Heterologous expression and functional properties of amiloride high affinity (NHE-1) and low affinity (NHE-3) isoforms of the rat Na/H exchanger, J. Biol. Chem. 268 (1993) 16369–16377.

[15] F.H. Yu, G.E. Shull, J. Orlowski, Functional properties of the rat Na/H exchanger NHE-2 isoform expressed in Na/H exchanger-deficient Chinese hamster ovary cells, J. Biol. Chem. 268 (1993) 25536–25541.

[16] M. Kuwahara, S. Sasaki, S. Uchida, E.J.J. Cragoel, F. Marumo, Different development of apical and basolateral Na–H exchangers in LLC-PK_1 renal epithelial cells: characterization by inhibitors and antisense oligonucleotide, Biochim. Biophys. Acta 1220 (1994) 132–138.

[17] J. Orlowski, R.A. Kandasamy, Delineation of transmembrane domains of the Na^+/H^+ exchanger that confer sensitivity to pharmacological antagonists, J. Biol. Chem. 271 (1996) 19922–19927.

[18] B. Coupaye-Gerard, C. Bookstein, P. Duncan, X.Y. Chen, P.R. Smith, M. Musch, S.A. Ernst, E.B. Chang, T.R. Kleyman, Biosynthesis and cell surface delivery of the NHE1 isoform of Na^+/H^+ exchanger in A6 cells, Am. J. Physiol. 271 (1996) C1639–C1645.

[19] J. Noel, D. Roux, J. Pouyssegur, Differential localization of Na^+/H^+ exchanger isoforms (NHE1 and NHE3) in polarized epithelial cell lines, J. Cell Sci. 109 (1996) 929–939.

[20] E. Slepkov, L. Fliegel, Structure and function of the NHE1 isoform of the Na^+/H^+ exchanger, Biochem. Cell Biol. 80 (2002) 499–508.

[21] M. Chakraborty, D. Chatterjee, F.S. Gorelick, R. Baron, Cell cycle-dependent and kinase-specific regulation of the apical Na/H exchanger and the Na,K-ATPase in the kidney cell line LLC-PK_1 by calcitonin, Proc. Natl. Acad. Sci. USA 91 (1994) 2115–2119.

[22] L.J. Deftos, M.R. Lee, J.T.J. Potts, A radioimmunoassay for thyrocalcitonin, Proc. Natl. Acad. Sci. USA 60 (1968) 293–299.

Available online at www.sciencedirect.com
SCIENCE DIRECT
ELSEVIER
Peptides 26 (2005) 2616–2623
PEPTIDES
www.elsevier.com/locate/peptides

Isolation and characterization of a glycine-extended form of calcitonin receptor-stimulating peptide-1: Another biologically active form of calcitonin receptor-stimulating peptide-1

Takeshi Katafuchi, Kazumasa Hamano, Katsuro Kikumoto, Naoto Minamino *

Department of Pharmacology, National Cardiovascular Center Research Institute, 5-7-1 Fujishirodai, Suita, Osaka 565-8565, Japan

Received 25 March 2005; received in revised form 4 June 2005; accepted 6 June 2005
Available online 14 July 2005

Abstract

In this study, we isolated a peptide eliciting a potent stimulatory effect on cAMP production in LLC-PK_1 cells from acid extracts of porcine brain. By structural analysis, this peptide was determined to be a C-terminal glycine-extended form of calcitonin receptor-stimulating peptide-1 (CRSP-1-Gly). Synthetic CRSP-1-Gly enhanced the cAMP production in COS-7 cells expressing calcitonin (CT) receptor as strongly as CRSP-1. Measurement of immunoreactive (IR) CRSP-1-Gly by radioimmunoassay using the specific antisera against CRSP-1-Gly showed that a relatively high level (>1 pmol/g wet weight) of IR-CRSP-1-Gly was detected in the midbrain, hypothalamus, anterior and posterior lobes of pituitary, and thyroid gland, and the ratio of IR-CRSP-1-Gly to total IR-CRSP-1 varies from 0.02 to 0.35 in each tissue. These results suggest that CRSP-1-Gly is actually present in the tissues as one of major endogenous molecular forms of CRSP-1, and can regulate the cells expressing the CT receptor both in the central nervous system and peripheral tissues in a manner similar to that of CRSP-1. IR-CRSP-2 and IR-CRSP-3 are also present in the brain and other tissues, but their tissue concentrations are 33% on average and less than 3% that of total IR-CRSP-1, respectively.

Keywords: Calcitonin receptor-stimulating peptide; Glycine-extended form of calcitonin receptor-stimulating peptide; Isolation; Calcitonin receptor; cAMP; Radioimmunoassay

1. Introduction

We have reported the structure, tissue expression and biological activity of three calcitonin receptor-stimulating peptides (CRSPs) in the pig [10,12]. Among them, the biological features of CRSP-1 have been characterized in greater detail. CRSP-1 exists in the central nervous system (CNS), pituitary and thyroid gland, and stimulates the calcitonin (CT) receptor about 100-fold more potently than CT. These facts indicate that CRSP-1 is a strong and specific ligand for the CT receptor expressing both in the CNS and peripheral tissues.

CRSP-1 was isolated from acid extracts of porcine brain by monitoring cAMP production through the endogenously expressing CT receptor expressed in LLC-PK_1 cells [9,12,15]. In the preceding study of CRSP-1 purification, six major peaks of the cAMP producing activity were observed in CM-52 ion exchange chromatography of the strongly basic peptides prepared from the porcine brain extracts [12]. Among them, CRSP-1 was isolated from the sixth peak of the cAMP producing activity, while we have identified the first three peaks as calcitonin gene-related peptide (CGRP) and its related peptides by further purification and structural analysis. In the present study, we successfully purified a new biologically active peptide from the fractions corresponding to the fifth peak of the cAMP producing activity in the CM-52 ion exchange chromatography, and determined it to be a glycine-extended and non-amidated form of CRSP-1 (CRSP-1-Gly) by structural analysis. Here we report the

* Corresponding author. Tel.: +81 6 6833 5012x2507; fax: +81 6 6835 5349.
E-mail address: minamino@ri.ncvc.go.jp (N. Minamino).

0196-9781/$ – see front matter © 2005 Elsevier Inc. All rights reserved.
doi:10.1016/j.peptides.2005.06.004

purification and biological activity of CRSP-1-Gly. Tissue concentrations of immunoreactive (IR) CRSP-1-Gly in the porcine tissues were also measured using a specific antiserum and compared with those of IR-CRSP-1, IR-CRSP-2 and IR-CRSP-3.

2. Materials and methods

2.1. Peptides

CRSP-1 was synthesized as described previously [12]. CRSP-1-Gly, N-Tyr-CRSP-1[30–38]-Gly and N-Cys-CRSP-1[30–38]-Gly were custom synthesized by American Peptide Company (Sunnyvale, CA). N-Tyr-CRSP-2[29–37]-NH_2, N-Cys-CRSP-2[29–37]-NH_2, N-Tyr-CRSP-3[29–37]-NH_2 and N-Cys-CRSP-3[29–37]-NH_2 were custom synthesized by Peptide Institute (Osaka, Japan). The purity and amino acid sequence were evaluated and confirmed using C_{18} reverse phase HPLC, amino acid analyzer and protein sequencer.

2.2. Measurement of cAMP production

COS-7 cells and LLC-PK_1 cells were maintained as reported previously [12], plated at 100,000 cells/well on 48-well plates and cultured for 24 h. The porcine CT receptor cDNA ligated into pcDNA 3.1 expression vector (Promega, Madison, WI) was transfected into the COS-7 cells with Lipofectamine Plus (Invitrogen Life Technologies, Carlsbad, CA) according to the manufacturer's protocol [13]. Both LLC-PK_1 and COS-7 cells that were recombinantly expressing the CT receptor were washed twice with Dulbecco's modified Eagle's medium (DMEM)/Hepes (20 mM, pH 7.4) containing 0.5 mM 3-isobutyl-1-methyl xanthine (Sigma, St Louis, MO) and 0.05% bovine serum albumin (BSA), and incubated in the same medium for 30 min at 37 °C. The incubation medium was then replaced with 150 μl of medium, in which the sample of interest was dissolved, and further incubated at 37 °C for another 30 min. Aliquots (100 μl) of the incubation media were succinylated, evaporated, and then submitted to radioimmunoassay (RIA) for cAMP, as reported previously [12].

2.3. Isolation of CRSP-1-Gly

The basic peptide fraction (SP-III) with molecular mass of about 3 kDa was prepared from porcine brain extracts as described previously [12]. This strongly basic peptide fraction was subjected to carboxymethyl (CM) ion exchange chromatography (CM-52, 2.4 cm × 45 cm; Whatman, Clifton, NJ) eluting with a linear gradient elution of $HCOONH_4$ (pH 6.5) from 9 mM to 0.45 M containing 10% CH_3CN. In the course of the present purification, aliquots (1/2000) of all fractions were lyophilized, dissolved in 200 μl of incubation medium, and submitted to the measurement of the cAMP producing activity using LLC-PK_1 cells. The fractions eliciting cAMP-producing activity were pooled and re-purified by cation exchange high performance liquid chromatography (HPLC) (TSK-gel CM-2SW, 7.8 mm × 300 mm; Tosoh, Tokyo, Japan) eluting with a linear gradient elution of $HCOONH_4$ (pH 3.8) from 9 mM to 0.9 M containing 10% CH_3CN at a flow rate of 2 ml/min. The biologically active fractions were successively separated by reverse phase HPLC on a C_{18} column (218TP54, 4.6 mm × 250 mm; Vydac, Hesperia, CA), and on a diphenyl column (219TP5215, 2.1 mm × 150 mm; Vydac) using a linear gradient elution of CH_3CN from 10 to 60% in 0.1% trifluoroacetic acid (TFA) at flow rates of 1 and 0.2 ml/min, respectively. The amino acid sequence was analyzed with a Procise cLC protein sequencer (492, Applied Biosystems, Foster City, CA), and mass spectra were measured using a single quadrupole mass spectrometer with electrospray ionization source (SSQ 7000, Finnigan, San Jose, CA) as described previously [12].

2.4. Preparation of antisera against CRSP-1-Gly, CRSP-2 and CRSP-3

All experimental procedures were approved by the local animal experiments and care committee. Rabbit antisera were raised against CRSP-1[30–38]-Gly, CRSP-2[29–37]-NH_2 and CRSP-3[29–37]-NH_2, to each of which an N-terminal cysteine was added to facilitate specific conjugation to maleimide-activated keyhole limpet hemocyanin through the sulfhydryl group of cysteine (Pierce, Rockford, IL). New Zealand White rabbits (Japan SLC, Hamamatsu, Japan) were immunized by injecting 1 mg of each peptide-keyhole limpet hemocyanin conjugate emulsified in complete Freund's adjuvant, and antibody production was boosted by five additional injections of the antigen conjugate emulsion at 3-week intervals.

2.5. Measurement of IR-CRSP-1-Gly, IR-CRSP-1, IR-CRSP-2 and IR-CRSP-3 concentrations in the porcine brain, pituitary and thyroid gland by RIA

N-Tyr-CRSP-1[30–38]-Gly, N-Tyr-CRSP-1[24–38]-NH_2, N-Tyr-CRSP-2[29–37]-NH_2 and N-Tyr-CRSP-3[29–37]-NH_2 were each radioiodinated by the lactoperoxidase method, and each monoiodinated peptide was isolated by reverse phase HPLC. Approximately 1 g of porcine tissue was minced and boiled for 10 min in 5 ml of water. After cooling, water and acetic acid were added to a final volume and concentration of 10 ml and 1 M, respectively, and the boiled tissues were homogenized with a Polytron homogenizer. The homogenates were then centrifuged, and 1 ml of the resulting supernatant was lyophilized, dissolved in the 1 ml of RIA buffer (50 mM sodium phosphate (pH 7.4), containing 80 mM NaCl, 25 mM EDTA, 0.05% NaN_3, 0.5% BSA treated with N-ethylmaleimide, and 0.5% Triton X-100). An aliquot (100 μl) of the solution was submitted to each RIA, which was performed by the procedures described previously [12].

2.6. Characterization of IR-CRSP-1 and IR-CRSP-1-Gly in the porcine brain

The SP-III fraction of porcine brain extracts was lyophilized, dissolved in 60% CH_3CN containing 0.1% TFA and was equally divided into four portions. Each portion was separated by gel filtration HPLC (TSK-G2000 SW_{XL}, 7.8 mm × 300 mm; Tosoh) eluting with 60% CH_3CN containing 0.1% TFA at a flow rate of 0.2 ml/min, and the effluent was collected into the same tube set. One-fifth of each fraction was lyophilized, dissolved in the RIA buffer, and aliquots (100 μl) were submitted for RIAs for CRSP-1 and CRSP-1-Gly. The fractions containing IR-CRSP-1 or IR-CRSP-1-Gly were pooled, divided into two equal portions, and lyophilized. For the reverse phase HPLC, the half portion was dissolved in 10% CH_3CN containing 0.1% TFA and separated by a C_{18} column (Symmetry 300™ C_{18} 5 μm, 4.6 mm × 250 mm; Waters) using a linear gradient elution of CH_3CN from 10 to 60% containing 0.1% TFA at a flow rate of 1 ml/min. For the ion exchange HPLC, another half portion of the sample was dissolved with 9 mM $HCOONH_4$ (pH 6.5) containing 10% CH_3CN, and separated by CM ion exchange HPLC (TSK-gel CM-2SW, 7.8 mm × 300 mm; Tosoh) eluting with a linear gradient elution of $HCOONH_4$ (pH 6.5) from 9 mM to 0.9 M containing 10% CH_3CN at 2 ml/min. The whole fractions were lyophilized, eliminated $HCOONH_4$ by sublimation, dissolved in the RIA buffer (1 ml), and aliquots (100 μl) were submitted to RIAs for CRSP-1 and CRSP-1-Gly.

3. Results

3.1. Isolation and sequence determination of CRSP-1-Gly

Fig. 1A shows the absorbance and cAMP-producing activity of each fraction in the CM-52 cation exchange chromatography of the basic peptide fraction of about 3 kDa prepared from porcine brain extracts. At least six major peaks of stimulatory activity in the cAMP production assay were observed, and we previously purified peptides from peaks 1–3 and 6. Amino acid sequences of the peptides isolated from peaks 1–3 were determined from the N-termini to more than the 15th residues, which were identical with that of CGRP. Based on the sequencing data along with the elution positions of synthetic CGRP and its methionine sufoxide form in reverse phase HPLC, we deduced that three peaks eliciting the cAMP-producing activity were a methionine sufoxide form of CGRP, CGRP and an unidentified CGRP-derived peptide, respectively. On the other hand, CRSP-1 was isolated from peak 6 as shown in our preceding study [12]. The biologically active fractions corresponding to peak 5 were pooled, and first separated by CM ion exchange HPLC on a TSK-gel CM-2SW column using a buffer of different pH, and then purified by reverse phase HPLC on a C_{18} column. Final purification was performed by another reverse phase

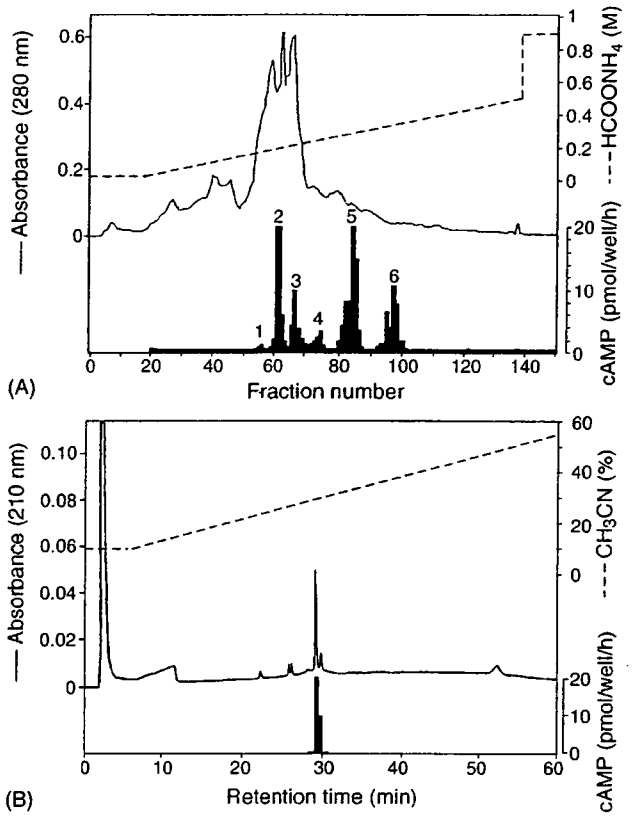

Fig. 1. Purification of CRSP-1-Gly from porcine brain extracts. (A) CM ion exchange chromatography of the basic peptide fraction prepared from porcine brain extracts. Sample: Basic peptides of molecular masses of 3 kDa obtained by successive Sephadex G-50 and G-25 gel filtrations from SP-III fraction of porcine brain extracts. Column, CM-52 (24 mm × 450 mm, Whatman); fraction size, 20 ml/tube; flow rate, 35 ml/h. Solvent system: linear gradient elution of $HCOONH_4$ (pH 6.5) from 9 mM to 0.45 M in 10% CH_3CN (v/v). (B) Final purification of CRSP-1-Gly by reverse phase HPLC. Sample: Biologically active fraction obtained by C_{18} reverse phase HPLC. Column, diphenyl (2.1 mm × 150 mm, Vydac 219TP5215); flow rate, 0.2 ml/min. Solvent system: Linear gradient elution of CH_3CN from 10 to 60% in 0.1% TFA (v/v) for 60 min. An aliquot of each fraction of (A) and (B) was submitted to the bioassay of cAMP producing activity in LLC-PK_1 cells.

HPLC on a diphenyl column, and the peptide was purified to a homogenous state (Fig. 1B).

To determine the amino acid sequence, intact and tryptic fragments of the purified peptide were subjected to the N-terminal sequence analysis using a protein sequencer. Contrary to our expectation, the amino acid sequences of the intact peptide and tryptic fragments were completely identical to those of CRSP-1, and the amino acid sequence of the purified peptide was confirmed up to the 37th residue. To determine the precise molecular mass, the purified peptide was analyzed using an ESI mass spectrometer, and its molecular mass was determined to be 4189.5 ± 0.3 Da. On the other hand, the molecular mass of CRSP-1 purified from peak 6 was determined to be 4130.6 ± 0.7 Da in the preceding study as two methionines of CRSP-1 (intact molecular mass 4098.9 Da) were oxidized to methionine sulfoxides (plus 16.0 Da × 2). As the difference of molecular